Available online at www.sciencedirect.com
ScienceDirect
Ceramics International 34 (2008) 351–357
CERAMICS INTERNATIONAL
www.elsevier.com/locate/ceramint

Photocatalytic performance and microstructure of thermal-sprayed nanostructured TiO_2 coatings

Zeng Yi [a,*], Juntao Liu [a], Wu Wei [a], Jianrong Wang [b], Soo Wohn Lee [c]

[a] *Shanghai Institute of Ceramics, Chinese Academy of Science, Shanghai 200050, China*
[b] *Jinan University, 106 Jiwei Road, Jinan 250022, China*
[c] *Sunmoon University, Department of Material Engineering, Asan, South Korea*

Received 20 February 2006; received in revised form 30 August 2006; accepted 20 October 2006
Available online 14 December 2006

Abstract

Titanium dioxide coatings were deposited by atmospheric plasma spraying (APS) with the use of agglomerated P25 powders and different spraying parameters (e.g. power) to determine their influence on the microstructure and photocatalytic performance of the coatings. The microstructure of as-sprayed TiO_2 coatings was characterized by scanning electron microscope (SEM), transmission electron microscope (TEM) and X-ray diffraction (XRD). The photocatalytic performance was evaluated by using methylene blue (MB) aqueous solution. The results showed that the power and flow of the secondary plasma gas have an important influence on the microstructure and on the anatase content of the TiO_2 coatings. Porosity is also a key factor in determining the photocatalytic performance of the TiO_2 coatings.

Keywords: Photocatalytic performance; Thermal spraying; TiO_2 coating; Microstructure

1. Introduction

Since Fujishima and Honda discovered the photocatalytic properties of TiO_2, a great deal of attention has been focused on applications of TiO_2 as a photocatalyst to solve environment problems [1–3]. Generally, there are two ways to apply a TiO_2 photocatalyst. One in the form of powder, and the other as coatings or films. Nanosized TiO_2 powders have been proved to possess good photocatalytic performance. The main problem with TiO_2 powders is how to collect the powder after use, otherwise the powder itself represents a pollutant. Thus, more interest is now focused on the preparation of coatings or films. The most common TiO_2 coating technologies are sol–gel processes, chemical vapor deposition (CVD), physical vapor deposition (PVD) and thermal spraying [4,5]. The thermal spraying process has many advantages, including its low cost, thicker coatings that can be formed quickly, a wide selection of materials, and a process that is simpler than other coating processes. Therefore, thermal spraying is considered to be the optimal method for producing TiO_2 photocatalytic coatings in most industrial applications.

In this paper, nanostructured TiO_2 coatings were prepared by the thermal spraying technology. The effect of the spraying parameters was studied. The microstructure of TiO_2 coatings was characterized by SEM, TEM and XRD. External bias was applied to the TiO_2 coatings in order to improve their photocatalytic performance.

2. Materials and experimental procedures

2.1. Feedstock powders

The feedstock powder used was commercial P25 TiO_2 powder (Degussa Corp., Germany). Fig. 1 shows the XRD pattern of P25 powder, which indicates that anatase is the main phase, representing approximately 83% as calculated from the XRD results [6]; rutile is the other phase. Fig. 2(1) shows TEM images of the initial nanosized starting powders. The average size was approximately 30 nm. However, this nanosized powder could not be fed directly into the plasma torch, so the TiO_2 powder was agglomerated by spray drying. After spray drying, the size range of the TiO_2 powder was approximately

* Corresponding author.
E-mail address: zengyi@mail.sic.ac.cn (Z. Yi).

0272-8842/$34.00 © 2006 Published by Elsevier Ltd and Techna Group S.r.l.
doi:10.1016/j.ceramint.2006.10.023

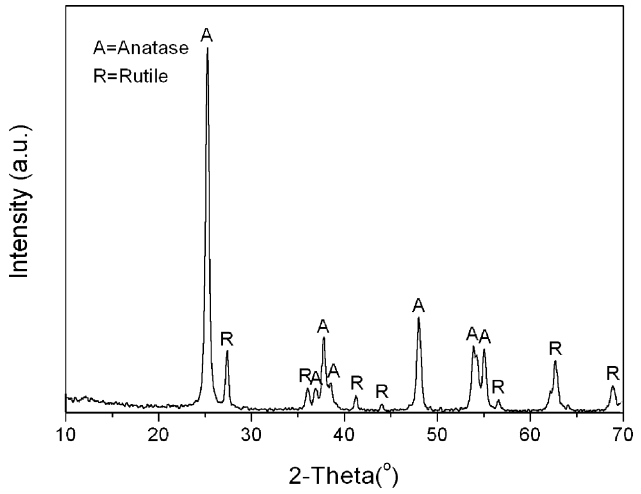

Fig. 1. X-ray diffraction pattern of starting TiO_2 nanopowders.

10–30 μm, as shown in Fig. 2(2). This was suitable for the thermal spraying process.

2.2. Plasma spraying equipment

An APS 2000 plasma spraying system F4-MB (Sulzer Metco Corp.) was used. To investigate the effect of the spraying parameters on the microstructure and properties of the coatings, five sets of parameters were selected. Table 1 shows the spraying parameters used to obtain the TiO_2 coatings.

2.3. Characterization of as-sprayed coatings

A JSM 6700F scanning electron microscope (SEM) with an Inca energy spectrum analyzer was used to obtain secondary electron (SE) images of as-sprayed anodes under different magnifications. The coating microstructure was analyzed with a JEM 2010F transmission electron microscope (TEM) operating at 200 kV. For the preparation of TEM samples, coatings were scratched from the substrate as a powder for observation. The X-ray diffraction (XRD) patterns of the samples were obtained with a Rigaku CN-2028 operated at 40 kV, 80 mA and Cu Kα radiation system.

Table 1
Plasma spraying parameters of TiO_2 coatings

	Coating				
	S1	S2	S3	S4	S5
Plasma gas (Ar) [SLPM]	40	60	40	40	80
Plasma gas (H_2) [SLPM]	12	12	4	12	6
Arc current [A]	605	604	705	424	303
Arc voltage [V]	68	66	55	68	76
Power [kW]	41	40	39	29	23

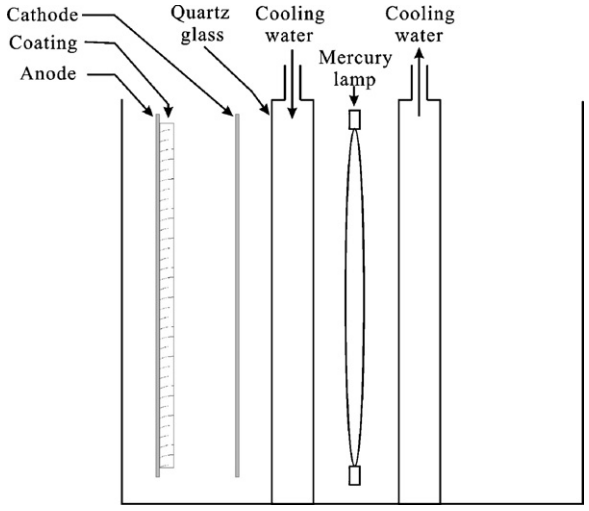

Fig. 3. Experimental apparatus for the photocatalytic reaction.

2.4. Photodecomposition testing

Methylene blue (MB) aqueous solution was used as the organic pollutant for photodecomposition evaluation, at a concentration of 10 mg/L. The concentration of MB solution can be measured by UV spectrophotometer (UV-1601PC, Shimadzu, Japan). A medium-pressure Hg ultraviolet (UV) lamp of 125 W (main wavelength of 365 nm) was used as the energy source for photoexcitation of the TiO_2 coatings. A schematic diagram of the photocatalysis experimental set-up is shown in Fig. 3. A perforated stainless steel sheet (pore size

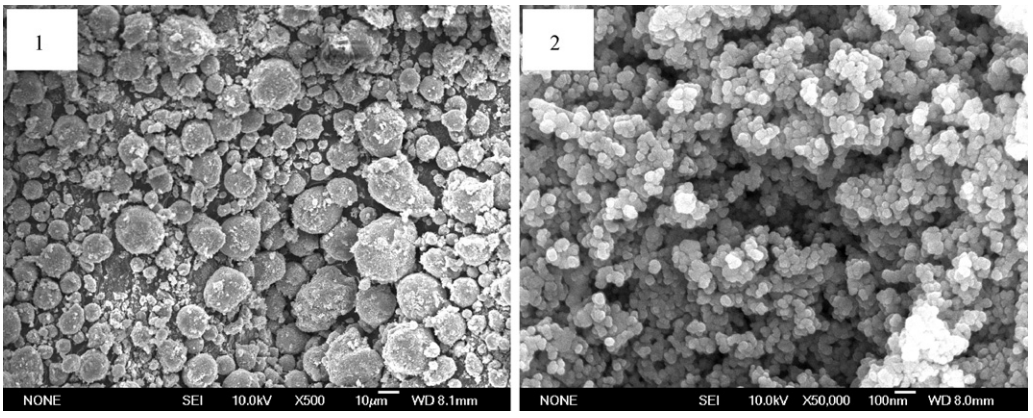

Fig. 2. Morphologies of starting TiO_2 nanopowders: (1) agglomerated and (2) primary powders.

approximately 1 mm) placed between the TiO_2 coating and the energy source was used as the cathode. The substrate was used as the anode. Thus, there was an electric field between the TiO_2 coating and the substrate. The photodecomposition efficiency η was calculated using the following equation:

$$\eta = \frac{C_0 - C_s}{C_0} \times 100\%$$

where C_0 is the original concentration of the MB aqueous solution and C_s is the concentration after UV irradiation.

3. Results and discussion

3.1. XRD analysis

Fig. 4 shows XRD patterns of the as-sprayed TiO_2 coatings for different spraying parameters. The phase compositions of all the coatings changed during the thermal spraying process. The major phase in all the as-sprayed coatings was rutile. The anatase content increased with decreasing flow rate of the secondary plasma gas (H_2). A new phase – the so-called magneli phase, besides anatase and rutile was also present [7]. The formation of the magneli phase may be related to TiO_2 reduction in the plasma torch. The temperature of the plasma torch is as high as 6000 °C and there are many H^+ ions, which can lead to TiO_2 reduction. Thus, molten titanium powder may react with H_2 during the plasma spraying process to form the magneli phase.

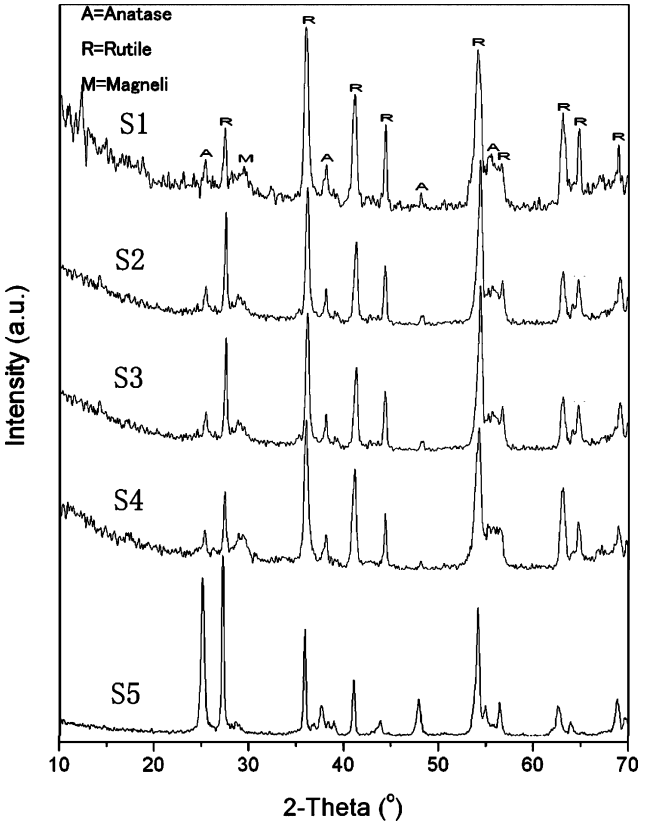

Fig. 4. XRD patterns of as-sprayed TiO_2 coatings.

Table 2
Average size and anatase content of as-sprayed TiO_2 coatings

	Coating				
	S1	S2	S3	S4	S5
Size of starting powders (nm)			30		
Grain size (nm)	61	70	56	47	32
Content (%)	11.5	13.7	25.4	13.5	41.6
Porosity (%)	2.8	14.6	11.4	10.5	29.2

Table 2 lists the content and average grain size of the anatase phase in the coatings. The grain size was calculated from the Scherrer equation. The anatase content is closely related to the secondary gas flow rate. Both S3 and S5 coatings with a lower H_2 flow rate contained more anatase phase compared with the other coatings. A lower H_2 flow rate would decrease the thermal conductivity of the plasma torch, so the temperature of the TiO_2 powder would be correspondingly low. The anatase phase, which is stable at temperatures below approximately 900 °C would transform to a stable rutile phase during the thermal spraying process.

3.2. Microstructure of as-sprayed TiO_2 coatings

Fig. 5 shows the surface morphology of as-sprayed TiO_2 coatings S1, S2 and S5. Both S1 and S2 show the typical microstructure of plasma-sprayed ceramic coatings. It is quite clear that they are formed by the buildup of successive layers of liquid droplets that flatten and solidify on impact to give a laminar microstructure. For the S5 coating, two types of structures are evident. One is a layer structure, which is similar to that of the S1 and S2 coatings. The other, which is the main structure, is a splat structure composed of nanosized particles. The average grain size of the S5 coating is 32 nm, which is similar to that of the starting powder. The morphology of the nanosized particles of the S5 coating is different to that of the S1 and S2 coatings. There are usually two types of particles in thermal-sprayed nanosized coatings. One is the unmelted starting powder, which retains the original particle size in the as-sprayed coating. The other is recrystallized grains that fully melt during the thermal spraying process. For recrystallized particles, the size distribution is narrower and more even. We suggest that the formation of nanosized particles in the S1 and S2 coatings is due to recrystallization, whereas that in the S5 coating is due to unmelted particles. As mentioned above, the lower H_2 flow rate for the S5 coating would result in a lower temperature of the plasma torch. Therefore, the S5 coating would possess more unmelted particles compared with the S1 and S2 coatings. For the S1 and S2 coatings, fully melted droplets recrystallized to form a nanostructure with an even distribution, which is confirmed by the SEM results.

Fig. 6 gives the cross-section morphologies of as-sprayed S1 and S5 coatings. The difference between the amounts of pores is quiet obvious. The porosities of as-sprayed coatings could be measured by LEICA Qwin image system.

As shown in Fig. 7, there are three types of grains. Most of them are the grains of 20–60 nm, as shown in Fig. 7(a), which is

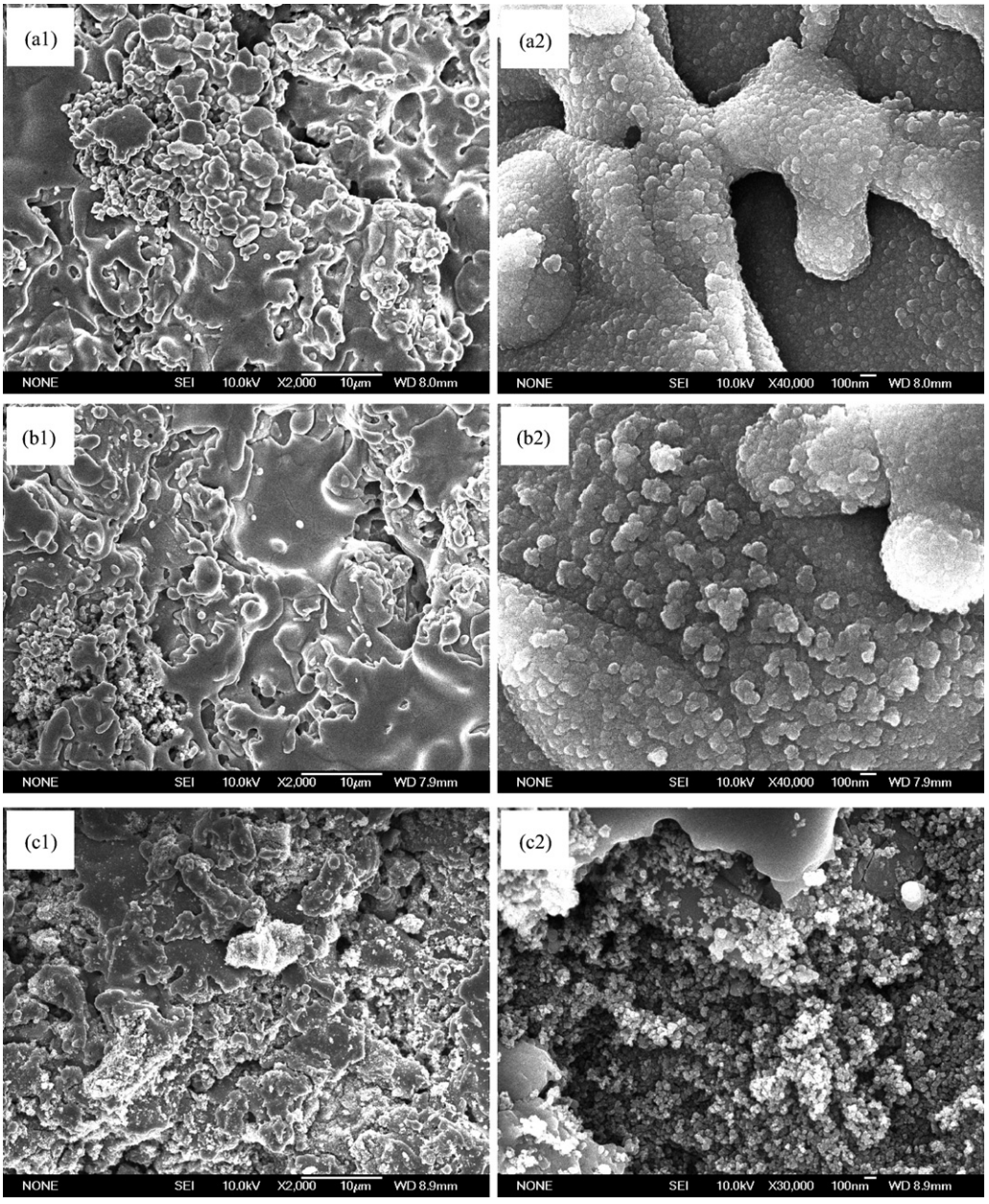

Fig. 5. Surface morphologies of plasma-sprayed TiO_2 coatings: (a1 and a2) S1; (b1 and b2) S2; (c1 and c2) S5.

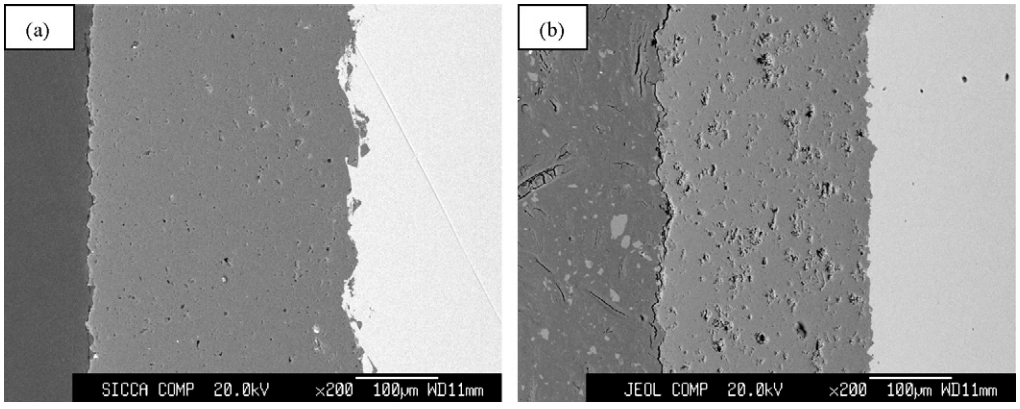

Fig. 6. Cross-section morphologies of as-sprayed coatings: (a) S1 and (b) S5.

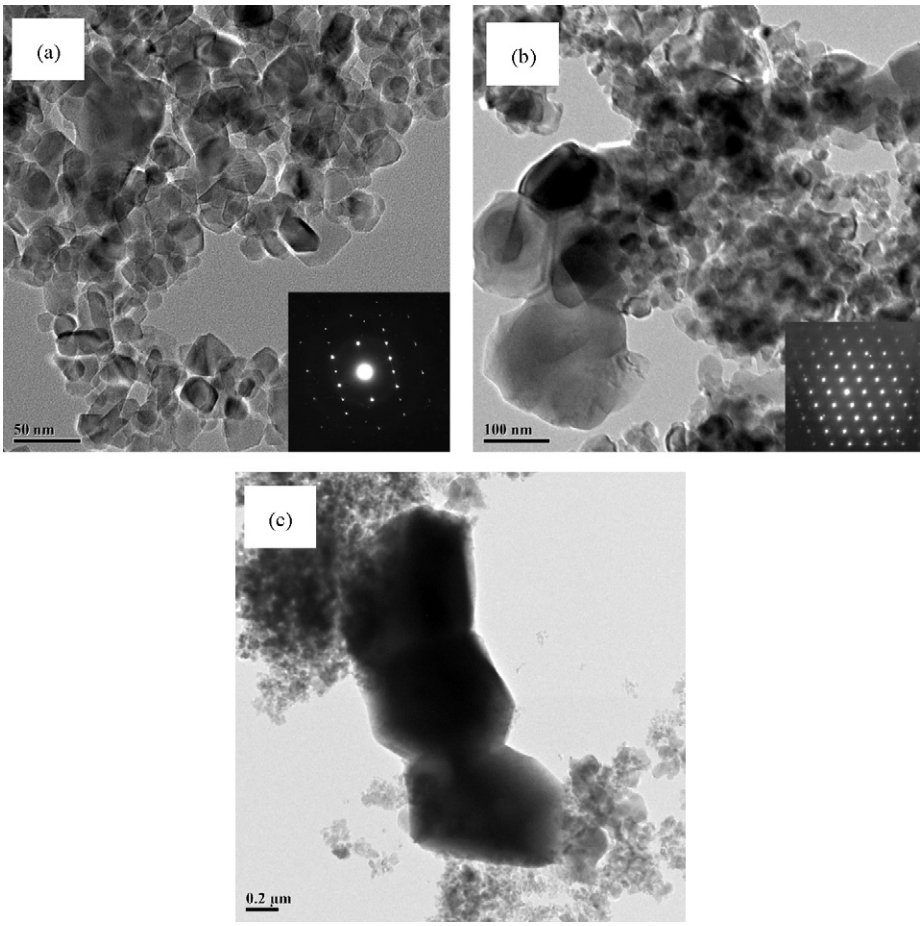

Fig. 7. TEM images of as-sprayed S5 coating.

in agreement with the SEM analysis. The SAD results show that the grains are anatase phase. There are still some grains of approximately 100 nm, which were confirmed as rutile by SAD, as shown in Fig. 7(b). The size of the largest grain is approximately 1–2 μm, as shown in Fig. 7(c), but the proportion of this type of grain is very small. SAD could not be carried out on such grains because of their thickness, but we can infer that these large grains are probably magneli phase.

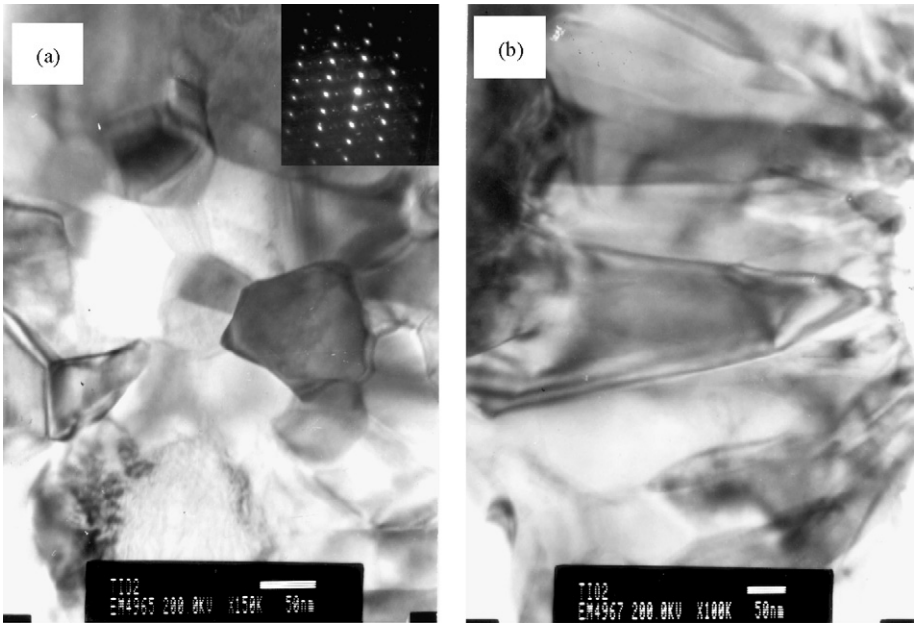

Fig. 8. TEM images of as-sprayed S1 coating.

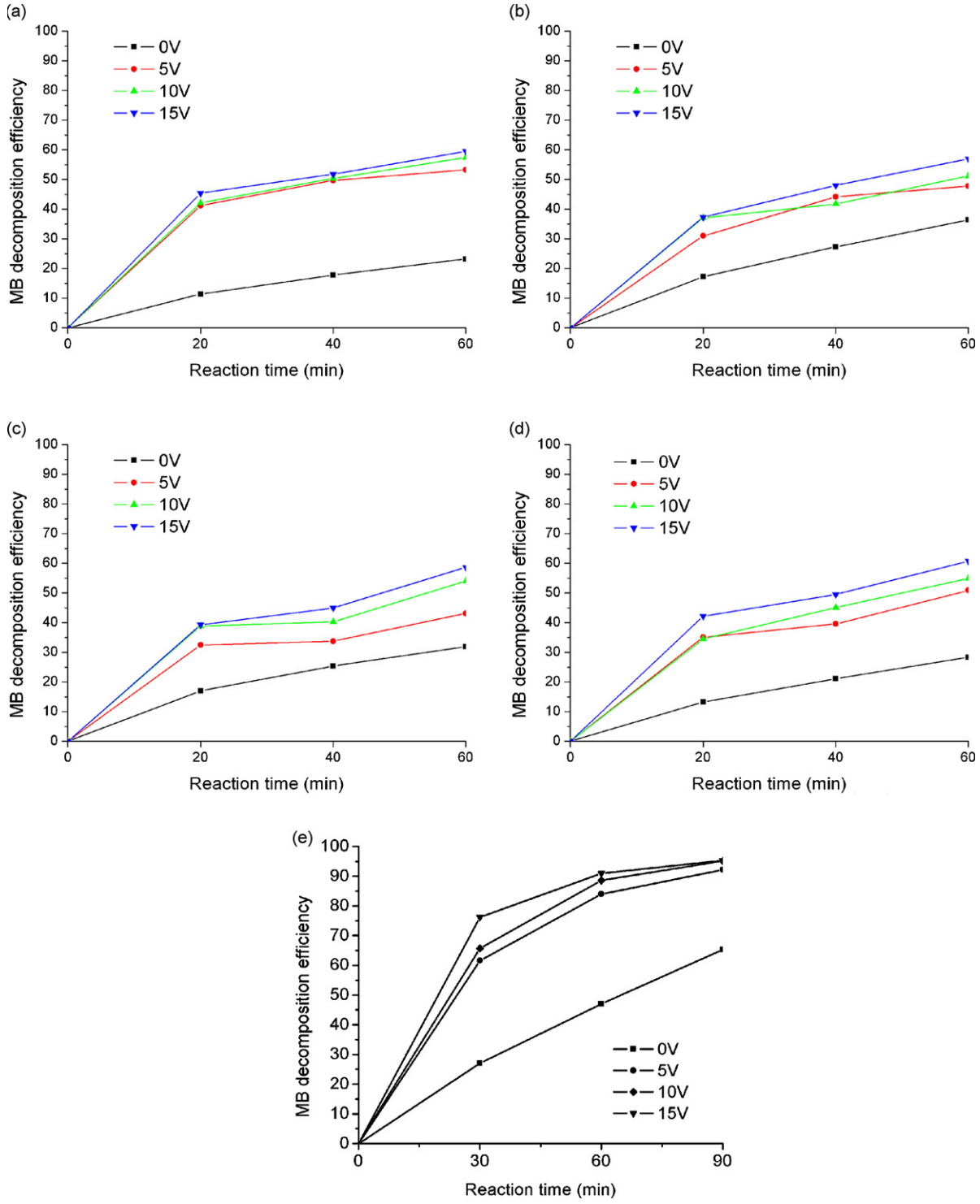

Fig. 9. Relationship between the photocatalytic efficiency and reaction time for as-sprayed TiO_2 coatings under different bias: (a) S1; (b) S2; (c) S3; (d) S4; (e) S5.

Fig. 8 shows TEM images of the S1 coating. The size of most grains in the S1 coating is less than 80 nm, and SAD confirmed that most of them are rutile, as shown in Fig. 8(a). This indicates that most of the grains transformed from anatase to rutile during the thermal spraying process. Some typical columnar crystals can be observed, which are perpendicular to the substrate, as shown in Fig. 8(b). The size of the columnar crystals is approximately 50 nm, which coincides with the grain size in the as-sprayed coatings measured by XRD. An increase in the temperature of liquid droplets, produced by the release of heat of fusion during rapid crystal growth, would tend to suppress further nucleation because of the large temperature dependence of the nucleation rate, and columnar crystal growth from the interface into the droplet would be thus expected.

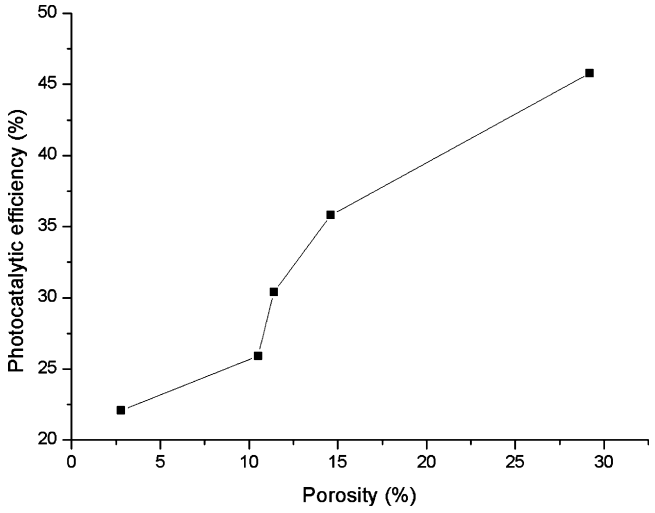

Fig. 10. Dependence of the photocatalytic efficiency on the porosity.

3.3. Photo-characteristics/decomposition

Fig. 9 shows the photodecomposition rates of the MB aqueous solution catalyzed by TiO_2 coatings prepared using different spraying parameters under different bias (0, 5, 10 and 15 V). When no bias was applied to the coatings, S5 showed the highest photocatalytic efficiency of up to 47%. The photocatalytic efficiencies for S1, S2, S3 and S4 were 25, 36, 32 and 28%, respectively. For all the coatings, the photocatalytic efficiency increased with increasing bias and reached a maximum at a bias of 15 V. In particular, for the S5 coating, the photocatalytic efficiency reached 91% when the bias was 15 V. The mechanism by which applied bias improves the photocatalytic performance of TiO_2 coatings has been discussed in our previous work [8].

The grain size and phase composition are the two key factors that determine the photocatalytic performance of TiO_2 coatings. According to Fujishima et al. [9], the reduction capability of anatase is stronger than that of rutile. Thus, anatase shows better photocatalytic performance because of its higher bandgap. Accordingly, the higher the anatase content, the better is the photocatalytic performance of the TiO_2 coating. It is easy to understand that the S5 coating showed much better photocatalytic performance than other TiO_2 coatings, regardless of whether voltage was applied or not.

Although the S1, S2, S3 and S4 coatings contain many nanosized particles, their average sizes are different, as shown in Table 2. The differences in photocatalytic performance, regardless of whether or not bias is applied, are not clear. Therefore, we can conclude that the grain size is not the most important factor that affects the photocatalytic performance of thermal-sprayed nanostructured TiO_2 coatings.

Porosity is another factor that affects the photocatalytic performance of TiO_2 coatings. Table 2 also lists the porosity of all the coatings. Fig. 10 indicates the dependence of photodecomposition efficiency under external bias of 15 kV on the porosity of TiO_2 coatings. It is evident that the efficiency improves as the porosity increases. The porosity has a great effect on the active area of as-sprayed coating: higher porosity results in a larger active area. Thus, the photodecomposition efficiency increases with increasing porosity. The S5 coating with many unmelted particles possesses higher porosity, so its photocatalytic performance would be best among all the coatings.

4. Conclusions

(1) The main phase composition changed from anatase in the powder to rutile in the coatings, and a new magneli phase appeared in the as-sprayed coatings.
(2) Both the anatase content and the microstructure are closely related to the flow rate of the secondary plasma spray gas and the power. There are many nanoparticles in all the as-sprayed coatings. However, the size and phase of these nanoparticles between S1 (high power) and S5 (low power) are different. The rutile phase is predominant at high spraying power, with a relatively larger size and more even distribution. The anatase phase is predominant at low spraying power because of the poor melting of particles.
(3) The coating obtained under the lowest power (S5) showed the best photocatalytic performance, regardless of whether or not an external bias voltage was applied. External bias voltage can improve the photocatalytic performance of thermal-sprayed TiO_2 coatings by retarding the recombination of electron–hole pairs. The porosity has a great influence on the photocatalytic performance of the coatings, whereas the grain size has little effect.

References

[1] A. Fujishima, K. Honda, Electrochemical photolysis of water at a semiconductor electrode, Nature 238 (1972) 37–38.
[2] A. Fujishima, T.N. Rao, D.A. Tryk, Titanium dioxide photocatalysis, J. Photochem. Photobiol. C: Photochem. Rev. 1 (2000) 1–21.
[3] G.H. Li, L. Yang, Y.X. Jin, L.D. Zhang, Structure and optical properties of TiO_2 thin film and TiO_2 + 2 wt.% $ZnFe_2O_4$ composite film prepared by r.f. sputtering, Thin Solid Film 368 (2000) 163–167.
[4] A. Ohmori, K.-c. Park, Electrical conductivity of plasma-sprayed titanium oxide coatings, Thin Solid Films 201 (1991) 1–8.
[5] F. Ye, A. Ohmori, The photocatalytic activity and photo-absorption of plasma sprayed TiO_2–Fe_3O_4 binary oxide coatings, Surf. Coat. Technol. 160 (2002) 62–67.
[6] R.A. Spurr, H. Myers, Quantitative analysis of anatase–rutile mixtures with an X-ray diffractometer, Anal. Chem. 29 (1957) 760–763.
[7] K.-W. Kim, E.-H. Lee, Y.-J. Kim, M.-H. Lee, D.-W. Kim, A study on characteristics of an electrolytic-photocatalytic reactor using an anode coated with TiO_2, J. Photochem. Photobiol. A: Chem. 103 (2003) 421–426.
[8] Z. Yi, W. Wei, J. Liu, Photo-decomposition property of thermal sprayed TiO_2 coatings, Mater. Sci. Forum 510–511 (2006) 26–29.
[9] A. Fujishima, K. Hashimoto, T. Watanabe, Photocatalytic Clean Revolution, Masao Kaneko, CMC, Tokyo, 1997 (in Japanese).